HIGH TEMPERATURE CO2RR ON YTTRIUM DOPED BARIUM ZIRCONATE ELECTROLYSIS CELL

A Thesis

Presented to the Faculty of the Graduate School

of Cornell University

In Partial Fulfillment of the Requirements for the Degree of

Master of Materials Science

By

Yucheng Zhu

August 2019

ABSTRACT

Modern society stands on fossil-fuel technologies. The electricity, heating, transportation, and entertainment derived from fossil fuels, while providing convenience to society, causes the CO_2 concentration in the atmosphere to rise, creating the greenhouse effect on the planet. CO_2 reduction reaction (CO2RR) is one of the potential methods to mitigate the greenhouse effect. Through CO2RR, CO_2 can be transformed into energy carriers such as CO, CH_4, C_2H_2, and others. Therefore, CO2RR can help to maintain the comfort of modern society while reducing the CO_2 emission. This thesis is based on experimental CO2RR studies carried out on a solid-state ionic device built from a Y-doped $BaZrO_3$ (BZY) perovskite. The main work is consisting of synthesis of BZY, construction of an anode-support proton conducting electrolysis cell (PCEC), X-Ray Powder Diffraction (XRD), Scanning Electron Microscope (SEM) characterization, and Electrochemical Impedance Spectroscopy (EIS) and high temperature CO2RR test. The results have shown that the CO2RR is feasible under the operating condition of the PCEC (350-450°C). Products including CO, H_2 and CH_4 were quantified using gas chromatography (GC). The project demonstrates the potential use of solid-state proton conductors for high-temperature CO2RR.

BIOGRAPHICAL SKETCH

The author, Yucheng Zhu, was born on January 3, 1995 in Jiangsu Province, China. He received a Bachelor of Materials Science and Engineering from Shanghai Jiaotong University in 2017. Currently, he is completing his MS program in Materials Science and Engineering Department at Cornell University.

This thesis is dedicated to my love.

ACKNOWLEDGMENTS

I am always on a journey. A journey to learn knowledge, a journey to dedicate myself and a journey to enjoy my life.

Cornell is a very important stop during my journey. Being abroad on my own for the first time in my life, it’s great to have people around me and help me go through this experience.

So much thanks for my advisor Pro. Jin Suntivich and Pro. Francis DiSalvo, my group members, all the people who have helped me.

TABLE OF CONTENTS

LIST OF FIGURES

Fig 18 Arrhenius Plot of CO2RR (a) Arrhenius Plot of transformation between CO_2 to CH_4 (b) Arrhenius Plot of transformation between CO_2 to CO (c) Arrhenius Plot of transformation between CO_2 to H_2 (d) Activation energy calculated for each plot verse overpotential.

LIST OF TABLES

LIST OF ABBREVIATIONS

CO2 Reduction Reaction (CO2RR)

$BaZrO_3$ (BZO)

Solid Oxide Fuel Cell (SOFC)

Solid Oxide Electrolysis Cell (SOEC)

Hydrogen Evolution Reaction (HER)

Yttrium Stabilized Zirconium Oxide (YSZ)

$BaCe_{0.5}Zr_{0.3}Y_{0.16}Zn_{0.04}O_3$ (BCZYZ)

Yttrium Doped Barium Zirconate (BZY)

X-ray Powder Diffraction (XRD)

Scanning Electron Microscope (SEM)

Linear Sweep Voltammetry (LSV)

Electrical Impedance Spectroscopy (EIS)

Chronoamperometry (CA)

Gas Chromatography (GC)

Proton Conducting Electrolysis Cell (PCEC)

Energy Information Administration (EIA)

Strontium-Doped Lanthanum Manganite (LSM)

Chapter 1

Introduction

1.1 Background

Fossil fuels is such a common energy that we may easily fail to notice its existence. Actually, the phones we use, the cars we drive, the heater we warm and the electricity we utilize all rely heavily on fossil fuels. According to Energy Information Administration (EIA)'s data, over one hundred years, only petroleum, natural gas, and coal has provided 80% of the energy consumption in USA. In 2015, fossil fuels account for 81.5% of the annual energy consumption in USA.

There are so many reasons for our heavy use of fossil fuels. Above all, fossil fuels have huge energy density. For example, gasoline has an energy density of 45MJ/kg, which means a typical tank of gasoline has the same energy of 80000 iPhone 6 batteries. Another thing is convenience, considering it only costs five to ten minutes to fill a car while it may take three hours to fully charge a cell phone. Ultimately, fossil fuels offer us safety. The accident in Chernobyl could have smaller impact if Soviet had used coal instead of nuclear.

However, as every coin has its two sides, Fossil fuels also releasing significant amount of CO_2 and other greenhouse gas, roughly 57% of the total emission via combustion. With CO_2 concentration changed from 317ppm to 400ppm over the recent fifty years, global temperature has witnessed an increase of 0.8°C.[1] Besides from species extinction and weather change, which may not be so evident, sea level rise is one of the most catastrophic results brought by greenhouse effect. Shown in Fig 1[1] is a

map of the America. The red area will be submerged in water given an 80m sea level rise, which includes most big cities along east coast.

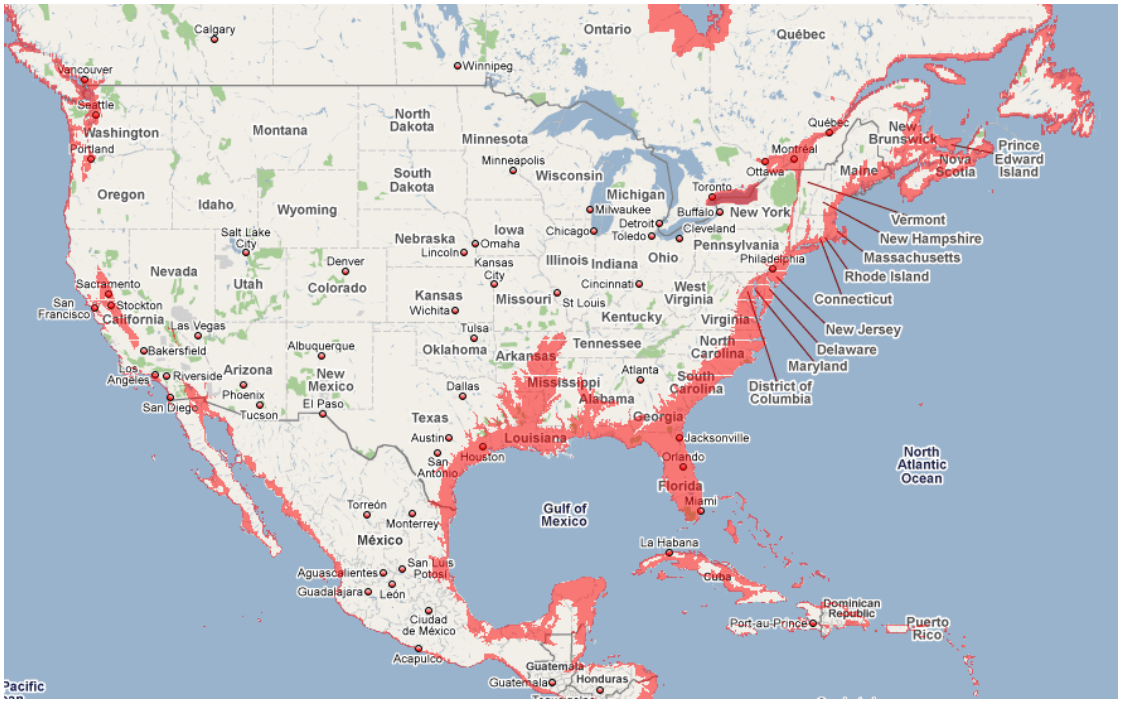

Fig 1 Map of America if sea level rises 80m. The red part will be submerged in sea.[1]

In order to avoid the catastrophe mentioned previously, great effort has been devoted into finding an alternative renewable energy for substitution of fossil fuels over the past two decades. Various kinds of renewable energy, like solar, wind and water, are studied and progress has been made. However, human still relies heavily on fossil fuels, as 80% of the energy consumed world-wide comes from fossil fuels. More importantly, considering the attributes of fossil fuels discussed above, there is hardly any new techniques can fully take place of fossil fuels. However, if we can combine new techniques together, we may be able to create a energy system which possess all the advantages of fossil fuels at 80% clip.

This idea inspires us to fulfill the artificial carbon cycle.[2] Fig 2 is a schematic description of artificial carbon cycle. A carbon cycle is where we combine hydrocarbons with oxygen to make CO_2, water and release energy via combustion. The energy can be used for different purpose: drive our cars, feed the plants and produce electricity. One of the most important steps of this loop is the transformation of CO_2 to other reusable fuel gases.

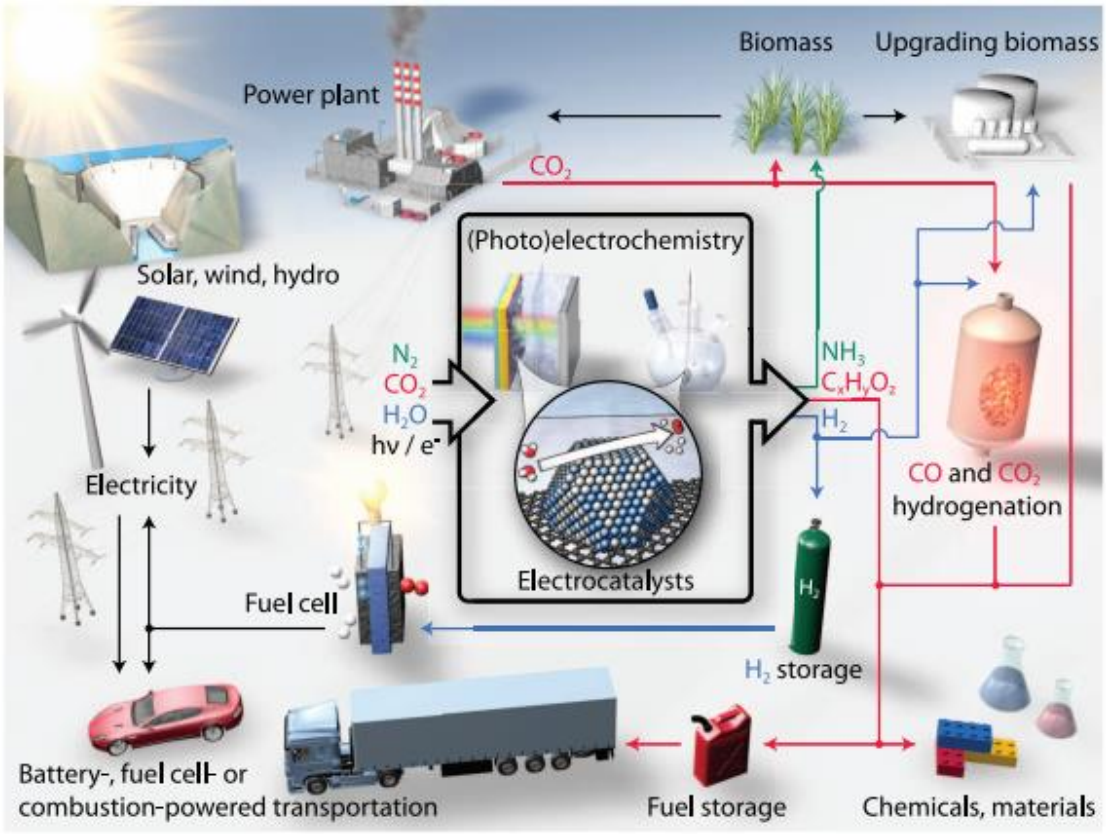

Fig 2 Carbon Cycle[2]

In order to fulfill this objective, scientists have developed several methods. First approach is biomineralization.[3] Different from human, some self-nourishing organisms are capable of fixing CO_2 and using it for the construction of their cell constituents. In general, these organisms can absorb the injected CO_2 and transfer it

into gas or oil reservoirs via biochemistry mechanism. However, the number of the organisms need to completely solve CO_2 problem is enormous and the performance of these organisms are heavily influenced by environmental factors, such as pH and atmosphere. For example, the well-known *Sporosarcina pasteurii* precipitate carbonate by saturation through urea hydrolysis, which is affected by environment pH. At the same time, the transportation of calcium, which is a necessary part for carbon fix is controlled by surrounding medium, other than pH.[4]

Another example is photochemical reduction[5], which typically involves solubilized molecules to produce stored chemical energy in the form of methane or other hydrocarbons from light energy. Basically, photochemical reduction is different from chemical reduction in that the electrons transferred are generated through the photoexcitation of a catalyst molecule, which also known as photosensitizer. After absorbing of light, the electrons are excited at the metal sites and move to functional ligands sites. Then, CO_2 interact with the reduced metal to form carbon products. Ultimately, photochemical reduction can achieve the goal to utilize solar energy to produce fuel gases. However, at present, since the efficiency of transferring solar energy is still low, a lot of work remains to be done before the fulfill of this objective.

Therefore, we would like to do the transformation electrochemically because this will allow us to fulfill CO2RR on industrial scale as well as using CO_2-free renewable energy, such as wind and solar. Electrochemical reduction of CO_2 can be split into two half reactions, one is water oxidation reaction at anode, another is CO_2 reduction reaction at cathode. This thesis is aimed at utilizing electrochemistry method to transfer CO_2 into fuel gases at high temperature.

1.2 Literature Review

1.2.1 Proton Conducting Perovskites

Perovskite is one kind of binary metal compounds which has a formula of ABC_3, where A and B represent cations and C represents anion. It has a typical cubic structure, shown in Fig 3.[6] Larger cation atom sits at the corner of the cubic while smaller cation is posited in the center of the C octahedron. Their properties in dielectric, piezoelectric, ferroelectric and pyroelectric make them a hot topic of research.[7,8]

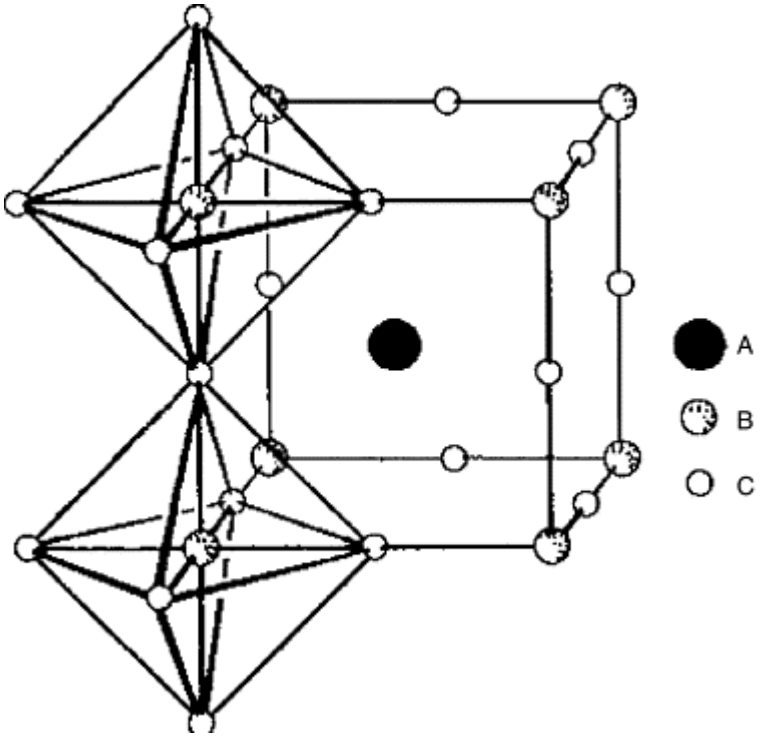

Fig 3 Crystal Structure of ABC_3[6]

Specifically, when C anion is an oxygen atom, the perovskite can conduct protons through the following equation:

$$V_{\ddot{O}} + H_2O \rightarrow 2H^+ + O_O^X \quad (1.1)$$

And the reaction constant is given by $K = \frac{[H^+]^2}{[P_{H_2O}]*[V_{\ddot{O}}]}$ (1.2)

$$2Zr_{Zr}^X + Y_2O_3 + O_O^X \rightarrow 2Y'_{Zr} + V_{\ddot{O}} + 2ZrO_2 \quad (1.3)$$

There are oxygen vacancies existing in the perovskites due to defects. Water in atmosphere will enter the oxygen vacancy and release protons. Considering equation (1.1) and (1.2), there are three ways to increase the proton concentration: The first one is by increasing temperature to increase the reaction constant. The second one is by increasing the humidity in atmosphere. And the last one is by adding dopants to create more vacancies through non-stoichiometric defects, shown in equitation (1.3) using the example of $BaZrO_3$(BZO).

People first found $SrTiO_3$, one kind of these perovskites, has conductivity about 10^{-3} S/cm scale around 1250°C in 1981.[9] Then, in 1985, Hagemann et al[10] found the same phenomenon in $BaTiO_3$ and proposed the defects mechanism shown previously to explain conductivity observed, motivating further investigation into barium-based perovskites area.

The second barium-based perovskites people looked into is $BaCeO_3$.[11] Though exhibiting a proton conductivity as high as 10^{-4}S/cm around 1250°C, $BaCeO_3$ is not stable in CO_2 containing atmosphere, which made people investigate another barium-based perovskite: $BaZrO_3$. Suzuki's group tested the proton conductivity of BZO and found it is little lower than BaCeO3.[12] This group also doped BZO with Yttrium, Dysprosium, Indium, Neodymium and Gallium and measured their proton conductivity. The results have shown that BZO doped with yttrium has the highest

proton conductivity among others with the same dopants' concentration. In 2007, the effect of yttrium concentration on BZO proton conductivity is reported by Yugami group.[13] In 0%mol-15%mol concentration range, they found the proton conductivity increases with the yttrium concentration, which can be explained by the increasing number of oxygen vacancies through equitation (1.3).

The findings about BZY attract much attention from scitentists. Further study carried out by Giuseppe Balestrino and Enrico Traversa[14] in 2010 testified the single phase BZO will be retained up to 50%mol dopants of yttrium. However, no increase in conductivity is observed when the concentration of yttrium is above 20%mol even though the proton concentration increases. The group also proposed a possible explanation for the reduction in conductivity. One reason is that with increasing yttrium sites, more protons are trapped, decreasing total mobility. Another is structural distortion caused by dopants, which cut off the transportation highways of protons.

Owing to the great performance perovskites possess, they have been already applied to construct solid oxide fuel cell (SOFC) and solid oxide electrolysis cell (SOEC). As early as 1982, Maeda et al have proposed the idea of building high temperature cell with perovskites to fulfill the transfer between electrical energy and chemically stored energy.[15] SOFC, as shown in Fig 4, composed of three parts: cathode, anode and electrolyte, all made up by solid ceramics, is able to generate electricity namely with oxygen and hydrogen with very little pollution. Through the transportation of oxygen ions in electrolyte layer. Specifically, if the conducting materials in the cell are proton conducting materials, the cell is called proton conducting fuel cell (PCFC). And over decades, there are many studies about PCFC based on different perovskites. For

instance, Professor O'Hayre's group from Colorado School of Mines reported the result of PCFC based on doped BZO tested in various kinds of fuel gases, including hydrogen, methane, domestic natural gas (with and without hydrogen sulfide), propane, n-butane, i-butane, iso-octane, methanol, ethanol and ammonia.[16] Great stability as long as 6000hrs is observed and high power density (0.8W/cm^2) is reported with hydrogen.

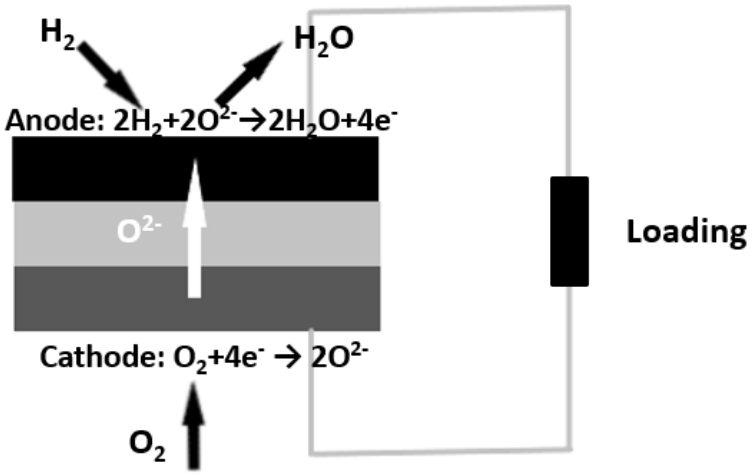

Fig 4. A schematic picture of SOFC

As mentioned above, perovskites can be used as the main materials for SOEC. A SOEC is a device, shown in Fig 5, the opposite of a SOFC, able to transfer electrical energy to chemically stored energy. [17] And with oxygen ions traveled through the electrolyte layer, we have oxygen formed on the anode and hydrogen formed on the cathode. Also, SOEC becomes a proton conducting electrolysis cell (PCEC) if the conducting materials in the cell are proton conducting materials. Due to high temperature perovskites can stand, water electrolysis on SOEC and PCEC has higher power and efficiency than room temperature one, making it the cheapest way to

produce hydrogen. At the very beginning, researchers focused on oxygen conductor like yttrium stabilized zirconium dioxide.[18]

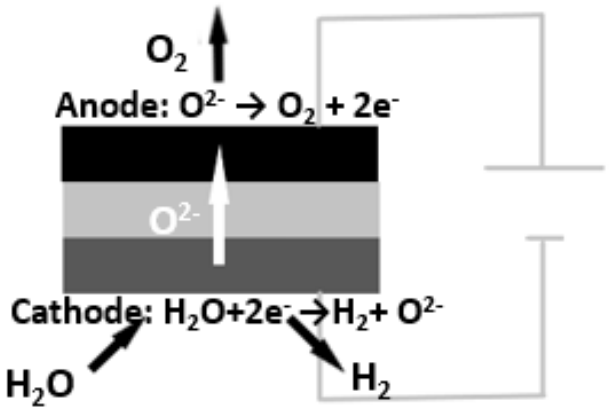

Fig 5. A schematic picture of SOEC

In 2002, Kobayashi et al successfully fabricated a PCEC based on Yb doped $SrZrO_3$.[19] Hydrogen as a product has been testified. More interestingly, the group managed to reduce NO using the same cell at approximately 460°C. In the comparison experiment, the group also substituted the electrolyte using yttrium stabilized zirconium dioxide but find no NO reduced. A possible explanation is that the proton in PCEC helps in the reduction of NO while oxygen ions show no effect. Shortly after Kobayashi's finding, a PCEC based on BZY is patented by Irvine et al[17], reporting the optimum thickness of the electrolyte to be 25um and optimum cathode to be porous Pt, which was confirmed one step further by Stuart et al[20]. Stuart's group also test the performance verse the dopants concentration and found that BZY with 10% dopants had the best performance.

For CO2RR, most of the studies done at high temperature is based on SOEC, shown in Table 1. However, the products are H_2 and CO with no hydrocarbon produced. A possible explanation for this phenomenon is that the conducting ions in SOEC is oxygen ions and protons cannot travel through the electrolyte to interact with CO_2 to form hydrocarbons.

Electrolyte	Cell Type	Products	Temperature	Overpotential	Reference
Ni doped Yttrium stabilized Zirconia	Button cell, electrolyte support	60%CO+40%H_2	800^{o}C	-1.1V	21
Yttrium stabilized Zirconia	Button cell, electrolyte support	100%CO	850^{o}C	-1.2V	22
Scandium stabilized Zirconia	Button cell, fuel electrode supported	73%H_2+27%CO	650^{o}C	-1.5V	23

Table 1 Studies on high temperature CO2RR using SOEC

1.2.2 CO2RR

People started looking into the electrochemistry to transfer CO_2 as early as 1985.[24] Electrochemical reduction of CO_2 possess several advantages which other methods discussed previously don't have, making it attract more attention from scientists. Above all, CO2RR is more controllable through changing temperature and overpotential. For another thing, most part of the system like a counter electrode, reference electrode and electrolyte can be reused, which makes CO2RR economically

and environmentally favorable. Ultimately, the electricity needed can be produced without generating new CO_2.

Despite the advantages above, the challenge remains, with the most severe one being the slow kinetics of the reaction. As mentioned previously, the electrochemical reduction of CO_2 can be split into two half-reactions: water oxidation which occurs at the anode and carbon dioxide reduction occurs at the cathode. Thermodynamically, water oxidation takes place at 1.23V/RHE and carbon dioxide reaction takes place at 0V/RHE. Unfortunately, CO_2 reduction is a difficult reaction and the reaction mechanism is complicated and still not fully clear today. However, the consensus has been reached that the first step is $CO_2 \rightarrow CO_2^{\bullet -}$. The potential for this reaction is -1.97V/RHE, which is a big energy gap. Excess energy is needed to make the reaction forward which is referred to as an overpotential. The fact that we are introducing excess energy makes CO2RR less efficient. Therefore, catalysts are used to decrease the overpotential needed. Besides, there exist many side reactions, making the product a mixture of CO, CH_4, CH_4O and so on, splitting which adds an unnecessary burden to the research.

To handle these two problems, scientists have spent over 20 years finding the suitable catalysts. A good catalyst should decrease the overpotential of the reaction, impede the formation of H_2 and be selective to one of the products.

People started their search from noble metals and found noble metals suitable for CO2RR.[25] For example, the well-known catalyst for Hydrogen Evolution Reaction (HER), Pt has been proved theoretically selective to methanol in acidic media in 2001,[26] while in electrolyte without water, oxalate becomes the main product

instead.[27] More interestingly, Centi et al found that Pt/C helps the formation of long carbon chain hydrocarbons (>C5).[28] However, these findings are mostly based on complicated processed or designed Pt, making it unrealistic for practical manufacture. What's more, due to Pt's high activity in HER catalysis, H_2 remains a significant part of the product. Ultimately, a common failure for noble metal is their high price, impeding their industrial utilization. Therefore, people start to look for common metal for substitution.

Unfortunately, most of the common metals have lower performance than noble metals. However, early research evidence shown copper being promising for CO2RR,[29] with CH_4 being the main product in aqueous potassium bicarbonate. Owing to the contribution of scientists all over the world, copper electrode has been well studied. Various products have been collected, including CH_4, C_2H_2, CO, HCOOH and even C6 long chain product.[30] Scientists have found that varying the reaction condition including temperature, electrolyte, overpotential and electrode structure can influence the product to a large extent.[25] Therefore, the copper catalyst is far from its optimize and needs further work for improvement.

Besides copper, people have also studied transition metal-based catalyst, carbon-based catalyst and other metal catalysts for CO2RR.[27]

1.3 Problem Statement

Despite all the progress made, there is still no 'perfect' catalyst found for CO2RR. Therefore, our group decided to study it from a new perspective. Going back to the fundamental principle of how catalysts work, shown in Fig 6, we found that catalysts are used to decrease the large energy barrier between the reactants and the transition

state. Then, a simple question arises: can we overcome this energy barrier by increasing temperature?

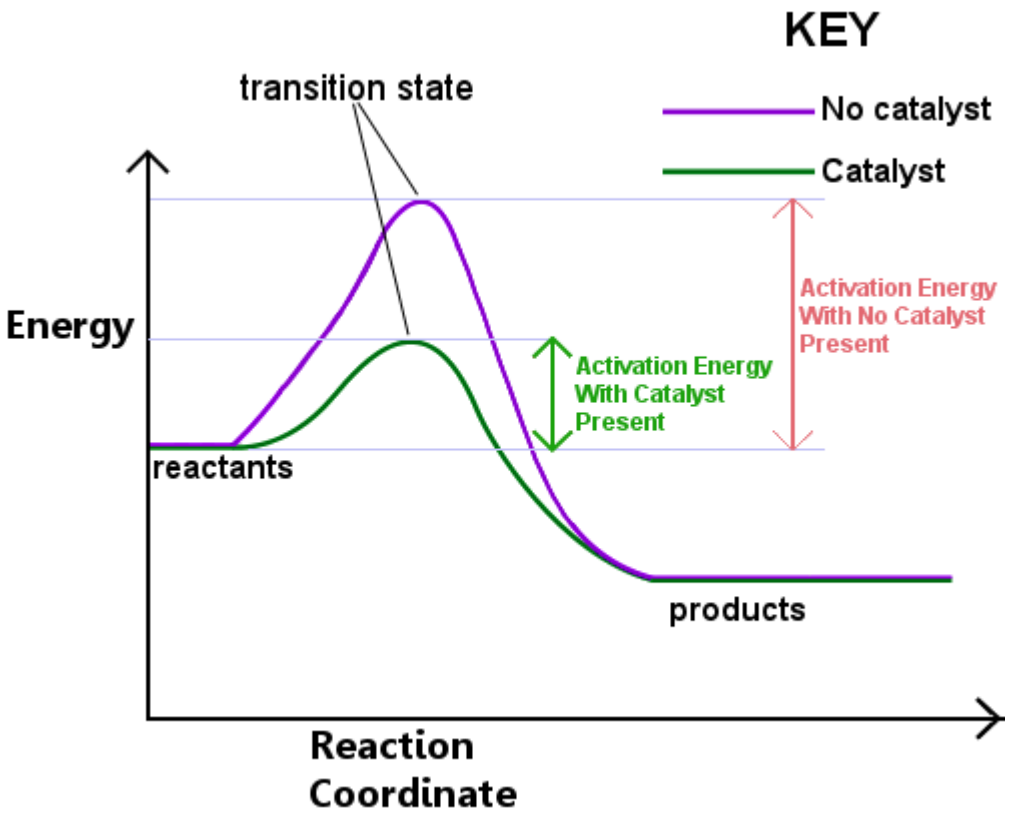

Fig 6. Working Principle of Catalyst

Conventional electrochemical reduction of CO2 is carried out in aqueous solution which restricts the reaction temperature to be lower than 100°C. Therefore, we consider using SOEC discussed previously to solve this problem.

As mentioned in Table 1, several researches have been carried out using SOEC for CO2RR. In 2008, Mogensen's group in Denmark build a SOEC and testified CO2RR is feasible on SOEC.[22] The cell had four layers: a Ni-Yttrium Stabilized Zirconium Oxide (YSZ) layer for mechanic support, a Ni-YSZ layer used as electrode, a YSZ electrolyte layer and a strontium-doped lanthanum manganite- YSZ layer as an

electrode. They examined the passivation rate of cell in different CO_2/CO compositions and found that the lowest passivation is achieved at CO_2/CO = 98:2, which is the industry grade. However, the only product is CO.

Then a hypothesis arises: is the failure of making hydrocarbons in SOEC due to the transportation ions are oxygen ions? In order to testify the hypothesis, we design a PCEC based on BZY, as shown in Fig 7. It has three layers: cathode, electrolyte and anode, all made up ceramics. Hydrogen oxidation reaction occurs at cathode while CO_2 reduction reaction occurs at anode. To the best of our knowledge, there is only one research about using PCEC for CO2RR. In 2011, Irvine et al reported reducing CO_2 into CO using PCEC based on $BaCe_{0.5}Zr_{0.3}Y_{0.16}Zn_{0.04}O_3$ (BCZYZ).[31] The anode used is Ni-BCZYZ composite materials and the cathode used is Fe-BCZYZ. The result has shown the main product is CO with small amount of CH_4 at 614°C. The group has achieved a total CO_2 conversion ratio up to 65%, indicating the feasibility of making hydrocarbons at high temperature using PCEC.

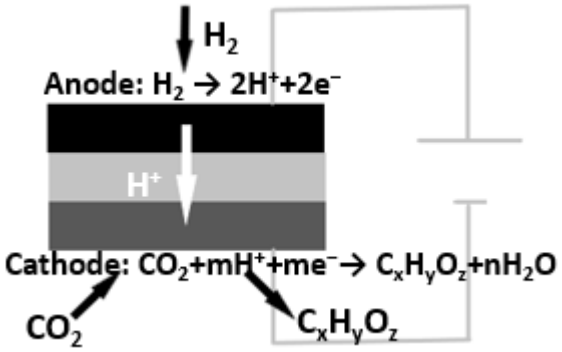

Fig 7. A schematic picture of PCEC used for CO2RR

1.4 Objectives

This thesis has two objectives:

1) Synthesis Yttrium doped Barium Zirconate with 20%mol dopant concentration
2) Build a PCEC using BZY and evaluate CO2RR performance of this cell

Chapter 2

Experimental techniques

2.1 Introduction

This chapter is composed of two small parts: sample preparation and characterization. The first part includes the synthesis of BZY, pellet cell design and fabrication methods. In the following part, we will discuss the techniques we apply to test the sample, including X-ray Powder Diffraction (XRD), Scanning Electron Microscope (SEM), Electrical Impedance Spectroscopy (EIS) and Chronoamperometry (CA).

2.2 Sample Preparation:

There are generally two methods for perovskites synthesis. One is wet chemical reaction and the other is solid state reaction. Wet chemical reaction can produce nanometer scale products but may introduce other impurities. This thesis employs solid state reaction of barium carbonate, zirconium dioxide and yttrium oxide to get high purity BZY. Chemicals used are: NiO (BTC) Y_2O_3 (Alfa Aesar) ZrO_2 (Spectrum) $BaCO_3$ (BTC) Polyethylene oxide (BTC) Ceramic Adhesive (Aremco)

BZY fine ceramic powder is synthesized through the following steps:

1. Measure appropriate amount of barium carbonate, zirconium dioxide and yttrium oxide and put them into mortars for ball milling.
2. Add milling balls into and then 5ml iso-propane alcohol into mortars.

3. Put the mortars into the ball milling device and ball mill for 24h
4. Put the samples into air furnace and sinter them at 1000°C for 10h

A rather lower temperature is used here for the sintering of precursors in order to get smaller products and prohibit coarser and more-agglomerated problems.

At first. We make electrolyte support cell which has a dense electrolyte layer for the mechanical support of the whole system. Its cross section schematic image is in Fig 8. The fabricated methods are below:

1. Press the fine BZY powder using Enerpac-Hydraulic-Press
2. Sinter the pellet at 1450°C in air furnace for 25 hours.
3. Clean the agate mortar with DI water, acetone, ethanol and iso-propanol.
4. Mix appropriate amount of previously mixed BZY and NiO powder, α-terpineol and oil turpentine in the agate mortar.
5. Brush the solutions on the sintered BZY-NiO pellet and sinter it at 1000°C for 10 hours.
6. Mixing appropriate amount of BZY powder with Cu powder and ball mill for 24 hours without solvents.
7. Clean the agate mortar with DI water, acetone, ethanol and iso-propanol.
8. Mix appropriate amount of BZY+Cu mixed powder prepared by step 6, α-terpineol and oil turpentine in the agate mortar.
9. Brush the solutions on the pellet sintered in step 5 and sinter it at 1000°C for 10 hours.
10. Put the cell in the center of two glass tubes and connect two glass tubes with Ceramic Adhesive

11. Sinter the whole device Fig 10 in 93°C for 2 hours and 260°C for 2 hours.

Fig 8 The schematic image of the cross-section of the electrolyte support cell

However, after several experiments, we find that resistance of the electrolyte is too high, which restricts the current density and increases the ohmic loss. In order to reduce the ohmic loss, we propose the anode support cell, shown in Fig 9.

Fig 9 The schematic image of the cross-section of the anode support cell

Fig 9 shows the schematic image of the cross-section of the anode support cell. The cell is composed of three layers: a dense anode layer for mechanical support, made up of mixed BZY and NiO powder, a thin electrolyte layer and a thin cathode layer. It is fabricated through the following steps:

1. Mixing appropriate amount of BZY powder with NiO powder and polyethylene oxide and ball mill for 24 hours without solvents.
2. Press the mixture of powder using Enerpac-Hydraulic-Press
3. Sinter the pellet at 1000°C in air furnace for 10 hours.
4. Clean the agate mortar with DI water, acetone, ethanol and iso-propanol.

5. Mix appropriate amount of BZY, α-terpineol and oil turpentine in the agate mortar.
6. Brush the solutions on the sintered BZY-NiO pellet and sinter it at 1450°C for 25 hours.
7. Mixing appropriate amount of BZY powder with Cu powder and ball mill for 24 hours without solvents.
8. Clean the agate mortar with DI water, acetone, ethanol and iso-propanol.
9. Mix appropriate amount of BZY+Cu mixed powder prepared by step 7, α-terpineol and oil turpentine in the agate mortar.
10. Brush the solutions on the pellet sintered in step 6 and sinter it at 1000°C for 10 hours.
11. Put the cell in the center of two glass tubes and connect two glass tubes with ceramic adhesive
12. Sinter the whole device Fig 10 in 93°C for 2 hours and 260°C for 2 hours.

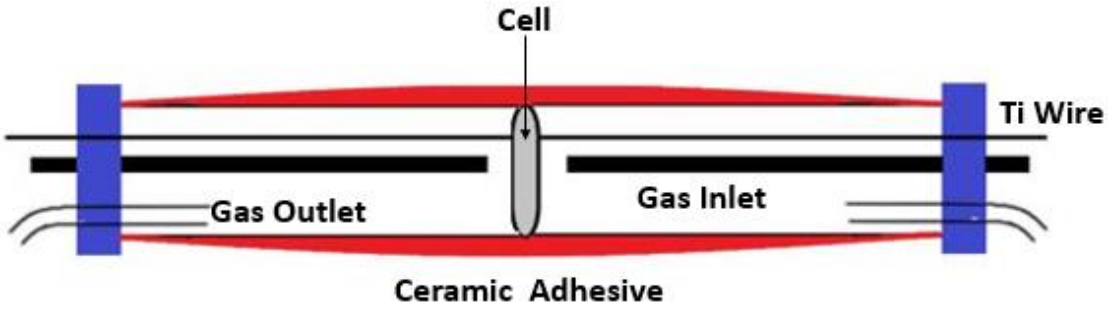

Fig 10 A schematic image of the PCEC device

Fig 10 shows how the PCEC device is made up. A two-chamber system is used here to ensure that two kinds of gases don't mix with each other. The previous fabricated anode support cell is in the middle of the two chambers with ceramic adhesive. Two

Ti wires are used to connect the cell to the potentiostat and each chamber has a gas inlet, which is a stainless-steel tube and a hole for gas outlet.

2.3 Sample Characterization

The x-ray diffraction is employed to examine the crystal structure of the synthesized BZY and BZO powder. The equipment used is a Rigaku Ultima IV diffractometer with a Cu kα x-ray wavelength of 1.5406 Å. The x-ray tube operates at 40KV and 44mA. The sample is scanned between 20°-100° range with 1°/min. The result is compared to ICDD data.

The SEM equipment is Zeiss Gemini 500 Scanning Electron Microscope. SEM is tested with a voltage of 8KV. The use of SEM helps us determine the thickness of three layers.

The EIS is measured using Pine WaveDriver 200 at 450°C 500°C 550°C 600°C, respectively. The EIS are used to determine the conductivity of the synthesized BZY with 20% Y dopants in the condition of Pt|BZY|Pt| in 0.15 atm H_2O N_2. The intercept on real axis is used to calculate the conductivity.

The CA of the cell fabricated above are measured using Pine WaveDriver 200 at 350°C, 400°C, 450°C, respectively. The CA is used to supply stable current for the CO2RR in the condition of H_2|NiO+BZY|BZY|Cu+BZY|CO_2. The overpotential used is 1.0V, 1.2V, 1.5V, 1.8V and 2.0V at 350°C, 400°C, 450°C, respectively. The result of the reduction of CO_2 is confirmed by gas chromatography (Multiple Gas Analyzer #5) (GC) made by SRI Instruments.

Chapter 3

Results and Discussion

3.1 Introduction

This chapter is composed of results of the experiments mentioned previously on the synthesized BZY with 20% dopants, including XRD, SEM, EIS, CA and GC data.

3.2 XRD Analysis

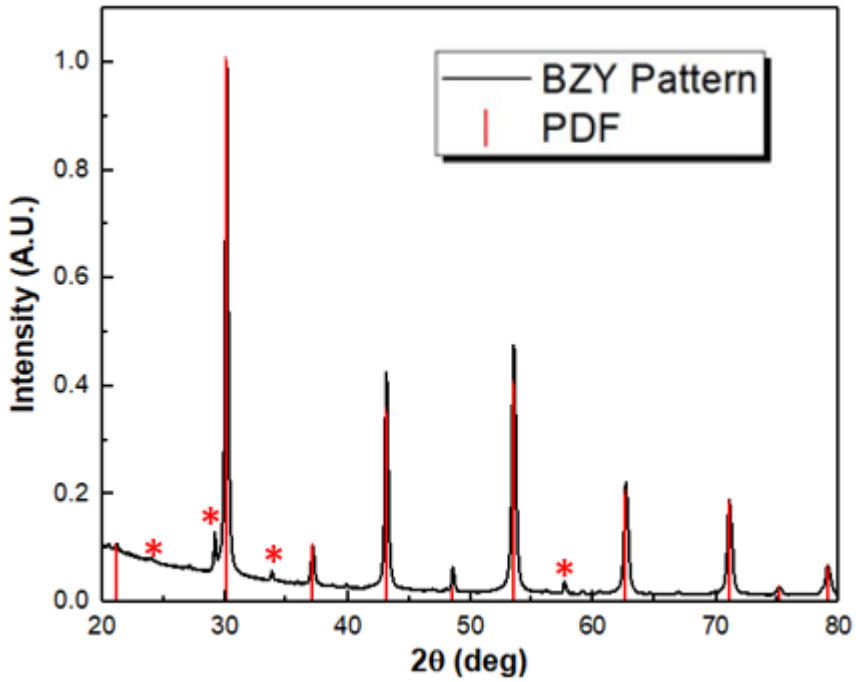

Fig 11 XRD pattern of BZY powder after mechanically grinding (Black) and PDF Data (Red) with red * indicating peaks of Y_2O_3

The first several times of the solid-state synthesis of BZY is not successful, as shown in Fig 11. The XRD pattern contains impurities of Y_2O_3, indicating not all Y atoms have entered Zr sites. Therefore, less oxygen vacancies and protons are produced through the non- stoichiometric reaction shown in equitation (1.3).

In order to figure out why the precursors remain unreacted, we investigate the reaction mechanism of the solid-state reaction and found that the synthesis of BZY is a diffusion-controlled reaction. Since the diameters of both barium atoms and zirconium atoms are large, the diffusion mechanism in BZY is through vacancy mechanism. Introducing a vacancy increases the volume of unit cell. Due to the close-packed structure, the energy needed for introducing a vacancy and moving a vacancy is huge. Therefore, the diffusion constant is small for BZY, making solid-state reaction often uncompleted. We can increase the diffusion constant by increasing temperature. However, it will also lead to coarser and more-agglomerated products. This is the reason we ball mill the reactants for 24hrs to mix them perfectly.

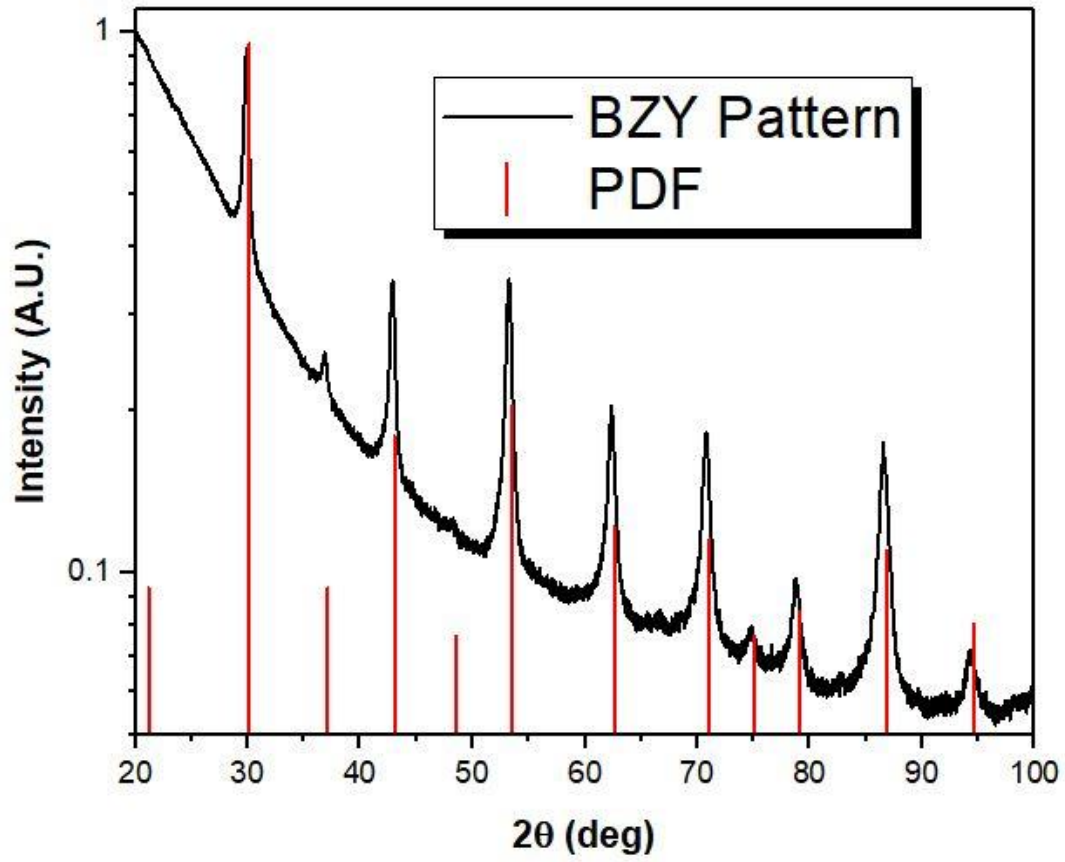

Fig 12 XRD pattern of BZY powder after ball milling for 24hrs (Black) and PDF Data (Red)

The XRD of synthesized BZY powder is shown in Fig 12. It shows clean BZY pattern meaning that our synthesis strategy is successful, and all yttrium atoms have entered the zirconium sites.

3.3 SEM Analysis

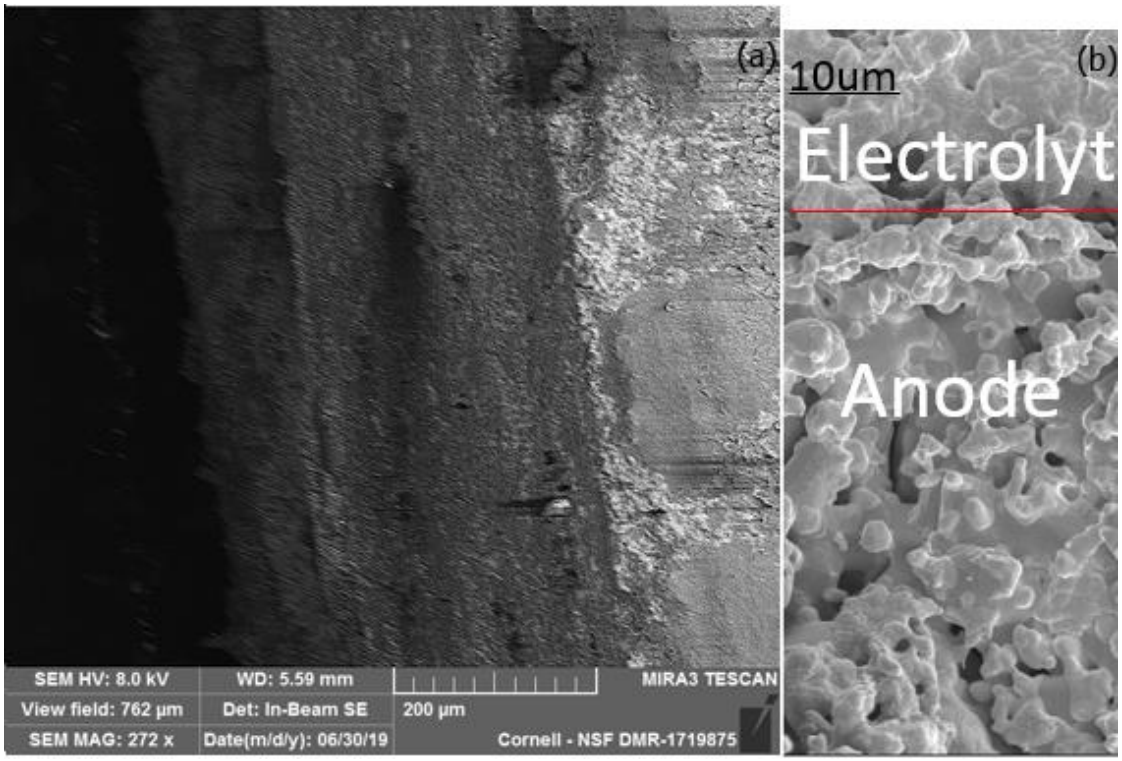

Fig 13 (a) SEM image of the cross-section of an anode support cell. (b) SEM image of the cross-section between electrolyte layer and anode layer.

Figure 13 is the SEM image of the cross-section of an anode support cell. The image on the right has shown two clear deviation lines between three layers: anode layer, electrolyte layer and cathode layer. The image on the left, with a higher resolution, shows that the polyethylene oxide used as binder which we put in during synthesis has

evaporated and the morphology of the anode thus becomes porous, which corresponds to our expectation since a porous anode layer is needed to let the gas permeate and provide more sites for the reaction. We have also confirmed that the thickness of the electrolyte and the cathode to be 200um and 100um, respectively. Compared to the electrolyte support cell, which normally has a thickness of 1500um, thickness of electrolyte in anode support cell is much thinner decreasing the resistance of the entire device.

3.4 Conductivity Analysis

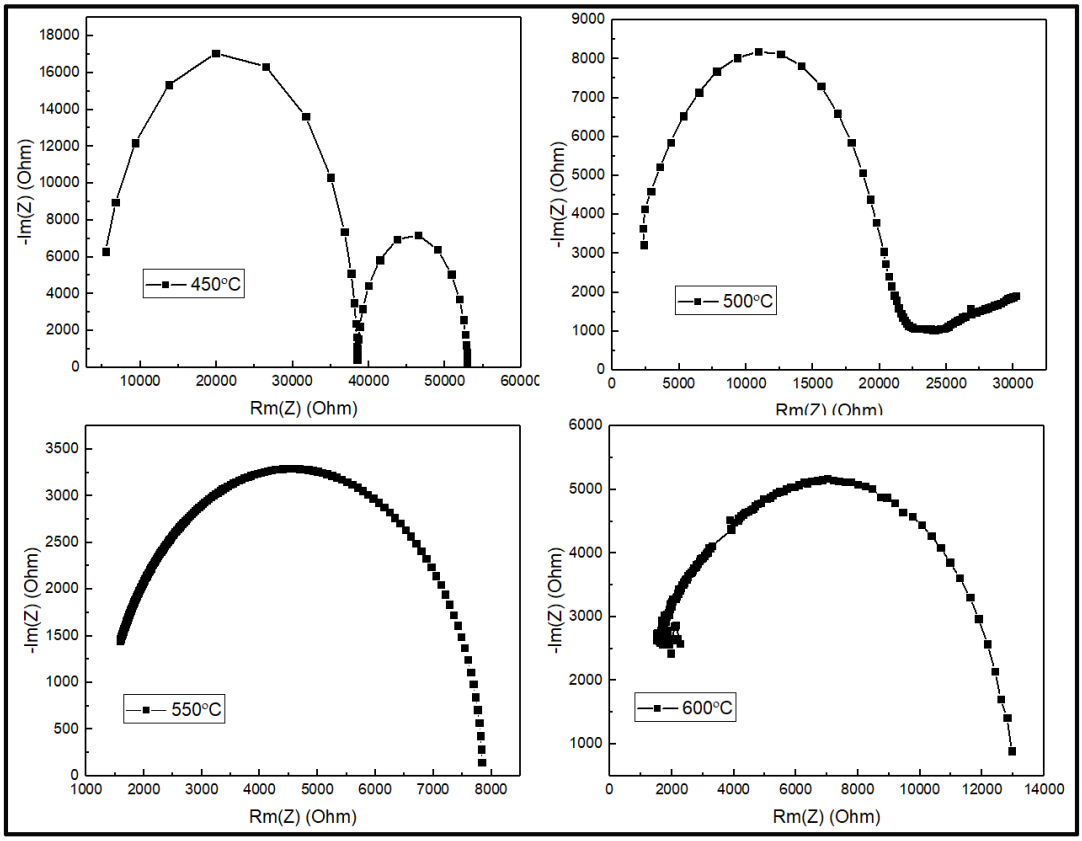

Fig 14 The Nyquist Plot of the BZY sample under four different temperatures.

The conductivity of BZY sample is measured under 0.15atm H_2O N_2 atmosphere in the form of dense pellet with Pt electrodes. Considering the water electrolysis reaction occurs at 1.23V/RHE thermodynamically, EIS is applied here to determine the true ohmic resistance. The data is collected from four temperatures: 450°C, 500°C, 550°C and 600°C, as shown in Fig 14. We assigned the intercept of the real axis at high frequency to be the resistance of the electrolyte. The specific conductivity of the electrolyte is calculated using the equitation below:

$$\sigma = \frac{L}{S \times R}$$

where L is the thickness the electrolyte layer, where S is the surface area of the cross-section of the electrolyte layer and R is the resistance got from the EIS data.

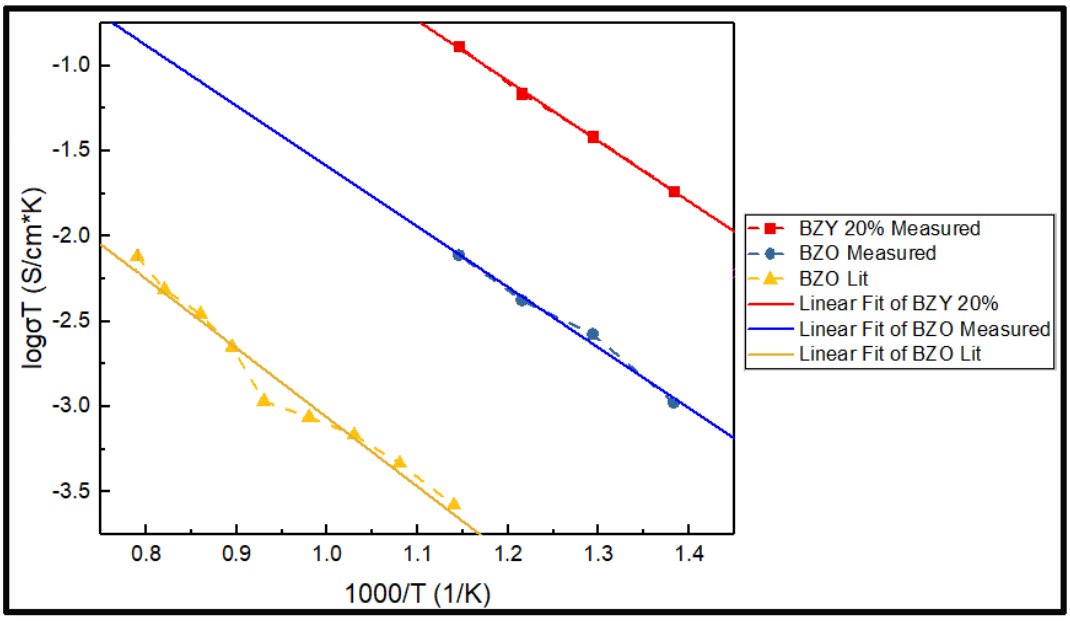

Fig 15 The total conductivity of the BZY and BZO sample and Lit data of BZO.[12]

The logarithm of the conductivity in different temperatures are plotted against 1000/T to construct the Arrhenius Plot, shown in Fig 15. The conductivity of pure BZO we measured is one magnitude higher than the lit data[12], which indicating our pellet has a better performance than lit. As mentioned before, the reaction temperature of BZO synthesis is 1000°C, lower than 1200°C-1350°C used by Suzuki's group.[12] Therefore, Suzuki's group's BZO powder is coarser and has more agglomerated problems than us. We also noticed that after the introduction of the dopants, the conductivity has increased by 2 magnitudes and is close to 10^{-2}S level, reported by Yugami et al.[13] The increase in conductivity is expected since more oxygen vacancies are created through the non-stichometry defect shown in equitation (1.3).

The Arrhenius Equitation shown below is used to calculate the activation energy of proton conducting.

$$\sigma = \frac{A}{T}\exp\left(\frac{-Ea}{KT}\right)$$

where A is a constant and T is the temperature while K is the Boltzmann constant. The activation energy is calculated to be 0.65eV for BZY and 0.72eV for BZO, respectively. These values are in reasonable range with the literature value of BZY and BZO to be 0.69eV and 0.8eV, respectively.[32] With the introduction of dopants, the activation energy of protons has been reduced. The decrease in activation energy comes from two reasons. For one thing, the increase of oxygen vacancy concentration makes the reaction shown in equitation (1.1) forward. For another thing, the proton travels in form of rotating hydrogen bonding. Thus, the dynamics of oxygen lattice has

great influence on the energy gap for protons' diffusion. With the introduction of Yttrium, more oxygen vacancies are created, increasing the average volume between oxygen atoms and decreasing the energy gap.

3.5 CO2RR Analysis

At first step, we test the electrolyte-support cell for CO2RR with a flow rate $1cm^3$/min in the setting below:

H_2|NiO+BZY|BZY|Cu+BZY|CO_2

The NiO+BZY is used as an anode while Cu+BZY is used as a cathode. With the flow of hydrogen on the anode side, NiO is reduced to Ni and able to conduct current. The I-V curve from CA plot and the product data from GC both are shown in Fig 16.

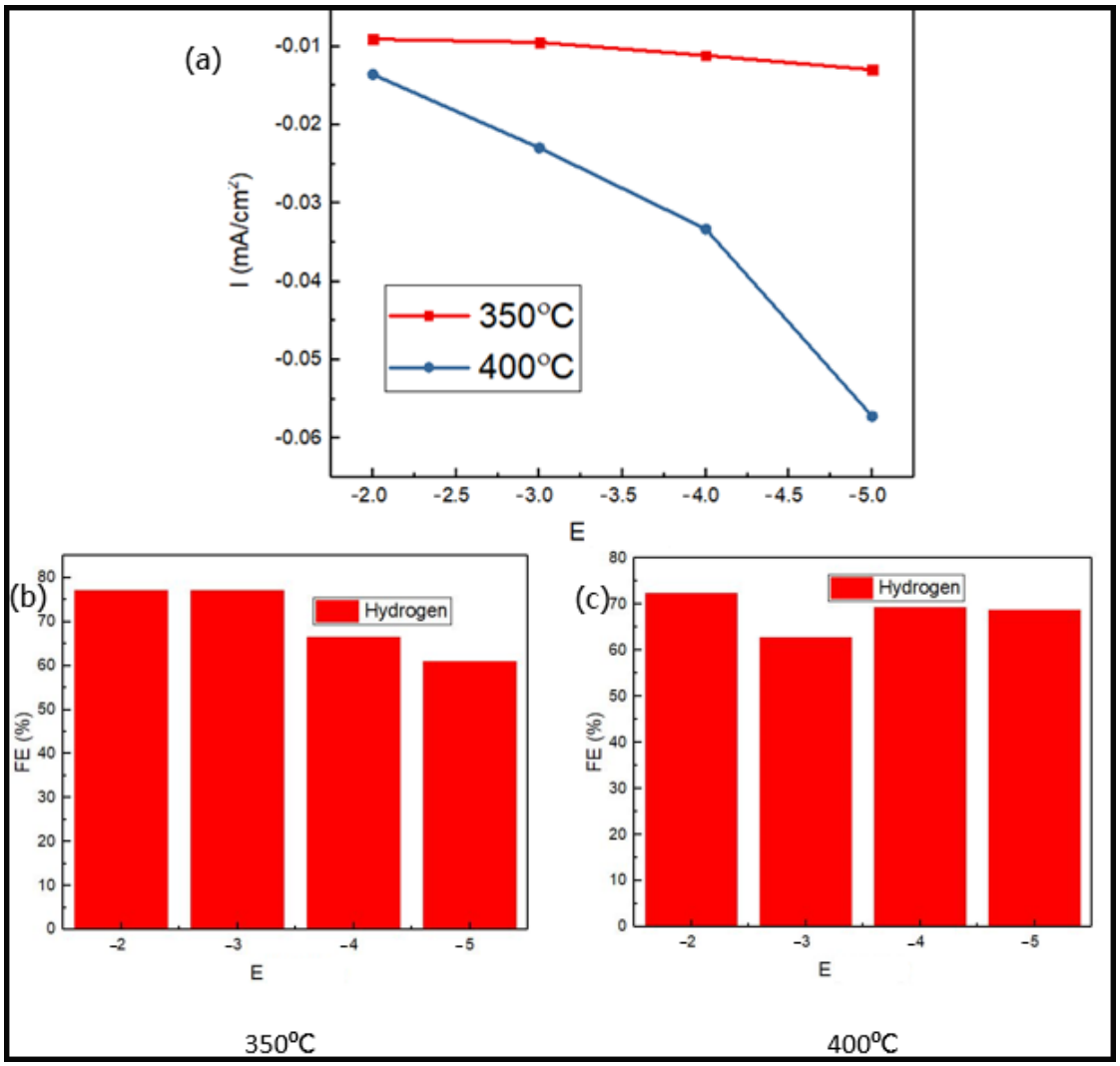

Fig 16 The performance of BZY electrolyte support cell. (a) current density verse overpotential applied (b) products at 350°C (c) products at 400°C. All E are in unit of V.

The current density is pretty low while the only product is hydrogen. We propose that the resistance of electrolyte is too high due to its thickness, inducing large ohmic loss. Therefore, the overpotential on cathode is too small to produce carbon products. In order to reduce the ohmic loss, we change our design to the anode support cell, shown

previously in Fig 9. The experiment system is the same as mentioned previously: H_2|NiO+BZY|BZY|Cu+BZY|CO_2.

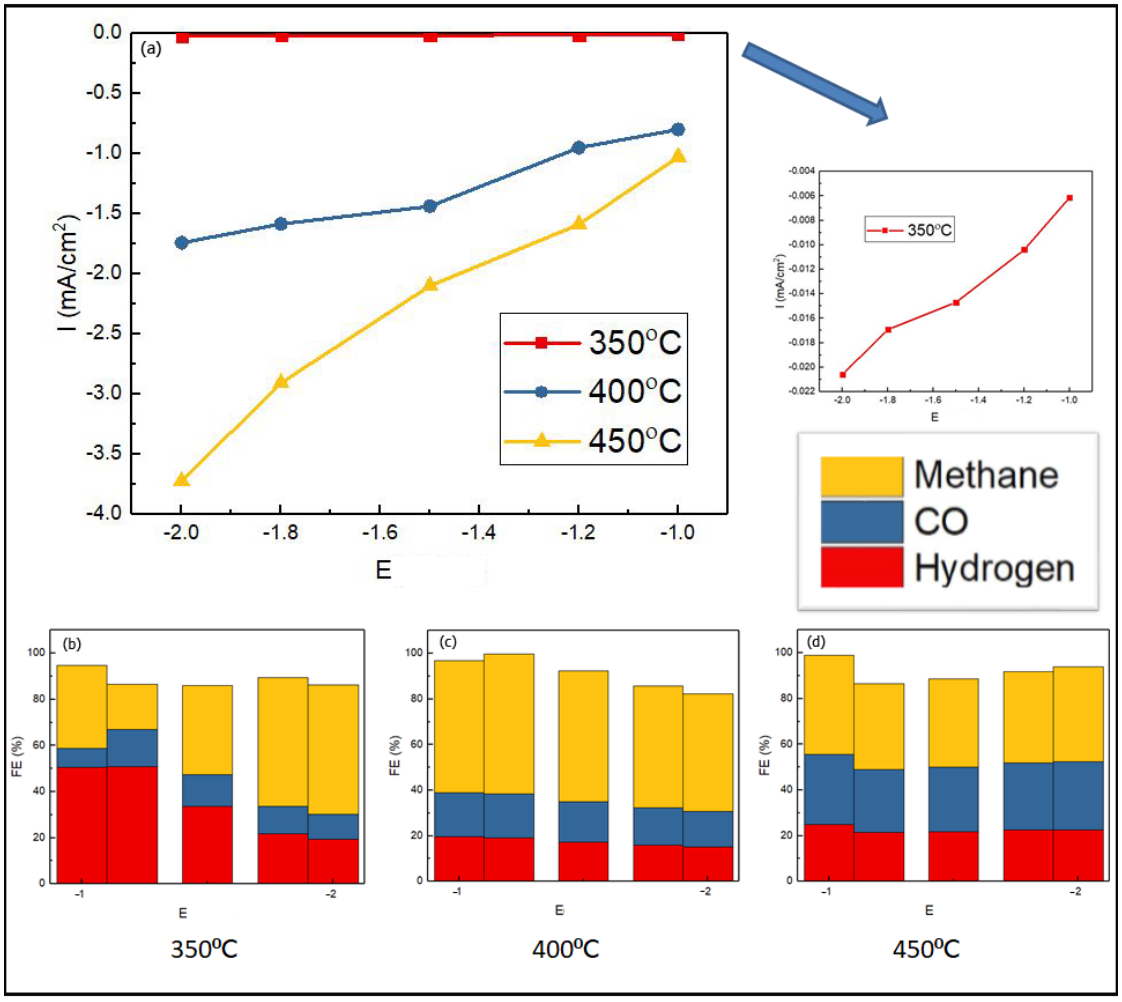

Fig 17 The performance of BZY anode support cell. (a) current density verse overpotential applied (b) products at 350°C (c) products at 400°C (d) products at 450°C. All E are in unit of V.

After applying the anode support cell, we have achieved 4mA/cm^2 current density at 450°C, which is much higher than electrolyte support cell, indicating reduction of the thickness of the electrolyte has decreased the resistance to a considerable extent.

Besides, the product has become mainly CH_4 with small amount of CO and H_2. The highest selectivity toward CH_4 product, which is about 60% is achieved at -1.2V 400°C.

Again, we plot the absolute current for each product verse 1000/T to construct the Arrhenius Plot. As shown in Fig 18 (a), (b) and (c), all plots are nearly linear, showing good Arrhenius behavior. Arrhenius Equitation below is used to calculate the activation energy for each product.

$$\mathrm{A} = \mathrm{C}\exp\left(\frac{-Ea}{KT}\right)$$

where A is the absolute current density for each product, C is constant, K is Boltzmann Constant and T is temperature

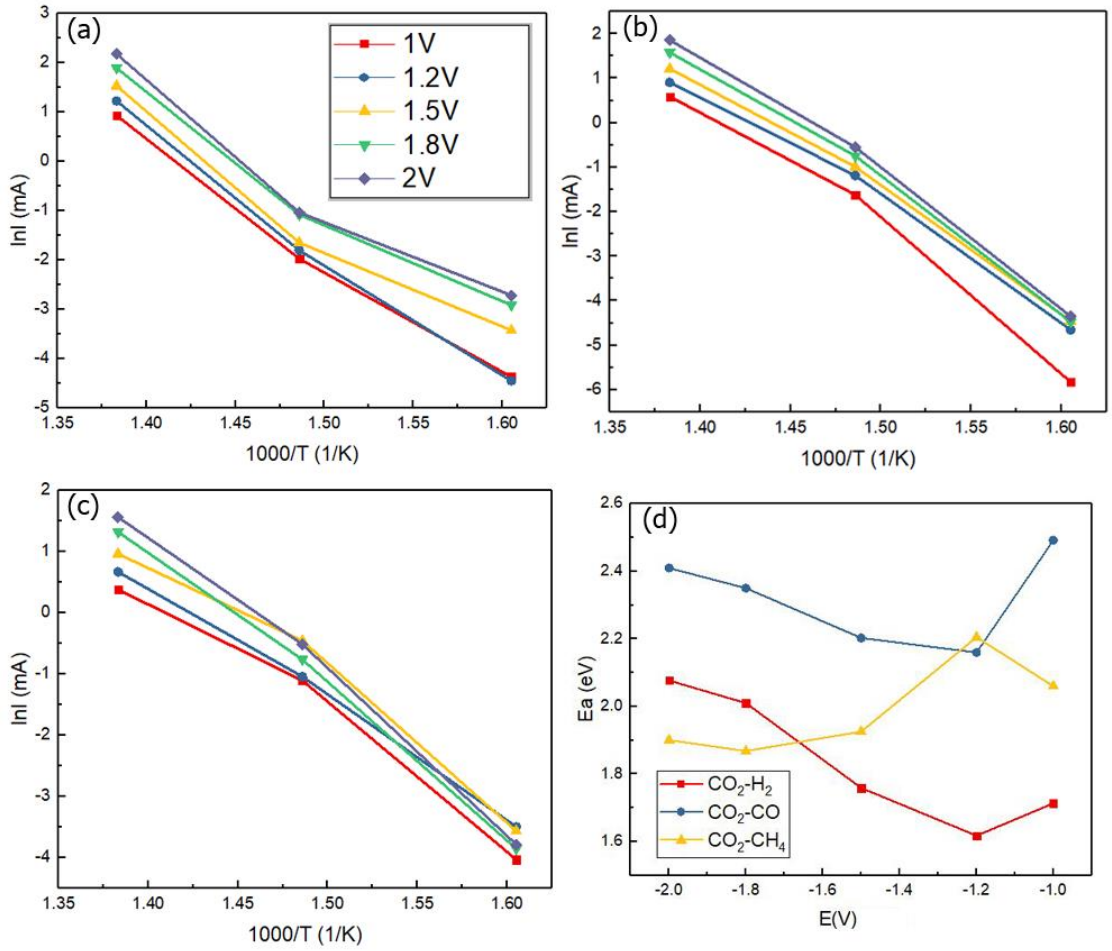

Fig 18 Arrhenius Plot of CO2RR (a) Arrhenius Plot of transformation between CO_2 to CH_4 (b) Arrhenius Plot of transformation between CO_2 to CO (c) Arrhenius Plot of transformation between CO_2 to H_2 (d) Activation energy calculated for each plot verse overpotential.

As shown in Fig 18 (d), CH_4 has the highest activation energy at -1.2V, making it less selective, corresponding to the highest CO and H_2 product amount at -1.2V shown in Figure 17 and the literature data.[33] With overpotential increases, CH_4 has become more kinetically favorable and selectivity toward CO and H_2 products decreases. That is because with the increase of overpotential, the intermediate of the CO_2-CH_4

transformation and the binding strength between the intermediate and the copper sites becomes more stable, which provides the chance for further reaction. Therefore, less CO is produced with increasing overpotential. At the same time, the hydrogen evolution reaction is blocked by two reasons. Firstly, the hydrogen evolution reaction is kinetically less favorable in high overpotential. What's more, due to more stable intermediate, CO_2 are consuming more protons and less proton can be provided for hydrogen formation. The failure to make higher hydrocarbons such as C_2H_4, which is produced at copper electrodes in aqueous electrochemical reduction, may be caused by lack of protons due to the low concentration of protons in solid electrolyte compared to liquid one.

Cell	CO	H2	CH4	T	E	I
NiO+BZY|BZY|Cu+BZY	32%	23.85%	44.15%	450°C	−2V	4mA/cm^2
NiO+YSZ|YSZ|LSM	100%	0	0	850°C	−1.2V	0.5A/cm^2
Ni+BCZYZ|BCZYZ|Fe+BCZYZ	86.8%	11.39%	1.7%	614°C	−2.5V	1.5A/cm^2

Table 2 Comparison of products with literature. [22,31]

Compared to lit, SOEC based on YSZ reported by K. Xie et.al.[31] produced only CO. As mentioned previously, the transportation ions in SOEC is oxygen ions. Few protons are provided to react with CO_2. Therefore, no hydrocarbon products are witnessed. Ebbesen et.al.[22] changed SOEC to PCEC and observed 1.7% CH_4 products. Considering Ebbesen's group did the experiment at 614°C, the low selectivity toward CH_4 may be caused by the decomposition of CH_4 at high temperature.
However, another possible reason exists as this small amount of CH_4 may come from the interaction between CO and H_2.

The failure for Ebbesen et. al.[22] to make hydrocarbons may be caused by two reasons. One of them being the instability of CH_4 in high temperature. Some of the CO product may come from the decomposition of CH_4. Another is the poor selectivity of Fe towards hydrocarbons, which has already testified by literature.[34]

We have also noticed that our current density is lower than literature. Apart from temperature's influence, here we propose a possible mechanism. In the first step, hydrogen is oxidized at Ni sites and protons are produced. Then, protons travel through the electrolyte via hydrogen bonding. Finally, when protons arrive at the cathode, they react with CO_2 to form hydrocarbons at copper sites. At the same time, electrons travel through the pathways formed by copper at cathode and Ni at Anode. If the BZY particles are too big, the pathways may be cut off and high ohmic loss is observed. Therefore, we are witnessing smaller current density compared to literature.

Though there is very little study about high temperature CO2RR. But here we propose a possible mechanism. The performance of PCEC in CO2RR is influenced by two main factors, one is electrolyte which determines proton mobility and concentration. Higher mobility or concentration can contribute to the formation of hydrocarbons. However, if the proton concentration becomes too high, protons mobility will be lowered by the trapping effect. Therefore, there is an optimize for the concentration and mobility. Another factor is functional metal cathode, as the reduction reaction occurs at cathode metal sites. The reaction pathway may be different from the aqueous one because the broken bonding is hydrogen bonding in PCEC while in aqueous electrolyte the broken bonding is O-H bonding. However,

discrete Fourier transform calculation is needed to figure the specific reaction pathways.

Chapter 4

Conclusion and Outlook

CO_2 reduction using solid proton conductor based on BZY is demonstrated by this work. This thesis focuses on the BZY with 20% Y dopants electrolyte and successfully fabricates an anode support PCEC. Single phased BZY has been synthesized and a close to literature conductivity is achieved. Compared to SOEC, the presence of H^+ can assist in the hydrocarbon production. The data from GC has shown that the products are CO, H_2, CH_4 and as high as 60% CH_4 product has been achieved. This work will work as a footstone for the high temperature CO2RR using SOEC. Further study may be carried out in the following directions:

1) Optimize the cell construction
2) Find the optimum condition of dopants
3) Fine the optimum catalyst
4) Use wet chemical reaction to produce nanometer scale BZY powder

There will be a long way to go before we solve all the questions above. However, we are one step closer to the truth.

Reference

[1] H. Ritchie and M. Roser, Publ. Online (2017).

[2] Z.W. Seh, J. Kibsgaard, C.F. Dickens, I. Chorkendorff, J.K. Nørskov, and T.F.

Jaramillo, Science (80-.). **355**, 146 (2017).

[3] S. Dupraz, B. Ménez, P. Gouze, R. Leprovost, P. Bénézeth, O.S. Pokrovsky, and F. Guyot, Chem. Geol. **265**, 54 (2009).

[4] J. Yoon, K. Lee, N. Weiss, Y.H. Kho, K.H. Kang, and Y. Park, Int. J. Syst. Evol. Microbiol. 1079 (2001).

[5] B. Kumar, M. Llorente, J. Froehlich, T. Dang, A. Sathrum, and C.P. Kubiak, Annu. Rev. Phys. Chem. **63**, 541 (2012).

[6] C. Li, K. Chi, K. Soh, and P. Wu, J. Alloys Compd. **372**, 40 (2004).

[7] W. Schattke, *Nanoelectronics and Information Technology Computational Methods for Large Systems The Physics and Chemistry of Nanosolids Introduction to Cluster Dynamics Advanced Calculations for Defects in Materials Handbook of Monte Carlo Methods* (Wiley, 2003).

[8] N. Setter, J. Eur. Ceram. Soc. **21**, 1279 (2001).

[9] M. Kakuchi, S. Sugawara, K. Murase, N. Chan, R.K. Sharma, and D.M. Smyth, J. Electrochem. Soc. **128**, 1762 (1981).

[10] J. Maier and W. Germany, J. Solid State Chem. **13**, 1 (1985).

[11] H. Iwahara, H. Uchida, K. Ono, and K. Ogaki, J. Electrochem. Soc. **135**, 3 (1993).

[12] H.Iwahara, T.Yajima, T.Hibino, K.Ozak, and IH.Suzuki, Solid State Ionics **61**, 65 (1993).

[13] F. Iguchi, N. Sata, T. Tsurui, and H. Yugami, Solid State Ionics **178**, 691 (2007).

[14] D. Pergolesi, E. Fabbri, A.D. Epifanio, E. Di Bartolomeo, A. Tebano, S. Sanna, S. Licoccia, G. Balestrino, and E. Traversa, Nat. Mater. **9**, 846 (2010).

[15] H. Iwahara, H. Uchida, and N. Maeda, J. Power Sources **7**, 293 (1982).

[16] C. Duan, R.J. Kee, H. Zhu, C. Karakaya, Y. Chen, S. Ricote, A. Jarry, R.O. Hayre, E.J. Crumlin, D. Hook, R. Braun, and P. Neal, Nature **557**, 217 (2018).

[17] T. Sakai, S. Matsushita, H. Matsumoto, and S. Okada, Int. J. Hydrogen Energy **34**, 56 (2009).

[18] M.A. Laguna-Bercero, J. Power Sources **203**, 4 (2012).

[19] T. Kobayashi, K. Abe, Y. Ukyo, and H. Iwahara, Solid State Ionics **155**, 699 (2002).

[20] P.A. Stuart, T. Unno, J.A. Kilner, and S.J. Skinner, Solid State Ionics **179**, 1120 (2008).

[21] P. Kim-lohsoontorn and J. Bae, J. Power Sources **196**, 7161 (2011).

[22] S.D. Ebbesen and M. Mogensen, J. Power Sources **193**, 349 (2009).

[23] W. Li, H. Wang, Y. Shi, and N. Cai, Int. J. Hydrogen Energy **38**, 11104 (2013).

[24] A. J.Bar, R. Parson, and J. Jordan, *Standard Potentials InAqueous Solution*, 2nd ed. (CRC Press, New York, 2017).

[25] B.R. Eggins and J. Mcneill, J. Electroanal. Chem. **148**, 17 (1983).

[26] G.M. Brisard, A.P.M. Camargo, F.C. Nart, and T. Iwasita, Electrochem. Commun. **3**, 603 (2001).

[27] J. Qiao, Y. Liu, F. Hong, and J. Zhang, Chem Soc Rev **43**, 631 (2014).

[28] G. Centi, S. Perathoner, G. Wine, and M. Gangeri, Green Chem **9**, 671 (2007).

[29] N. Hidetomo, I. Shoichiro, O. Yoshiyuki, I. Kazumoto, M. Masunobu, and I. Kaname, CSJ **63**, 2459 (1990).

[30] H. Shibata and J.A. Moulijn, Catal Lett **123**, 186 (2008).

[31] K. Xie, Y. Zhang, G. Mengb, and J.T.S. Irvine, J. Mater. Chem. **21**, 195 (2011).

[32] E. Fabbri, D. Pergolesi, S. Licoccia, and E. Traversa, Solid State Ionics **181**, 1043

(2010).

[33] M. Gattrell, N. Gupta, and A. Co, J. Electroanal. Chem. **594**, 1 (2006).

[34] A. Wifckowsi, E. Ghali, M. Szalarczyk, and J. Sobkowski, Electrochim. Acta **28**, 1619 (1983).